prolamine protein bodies.

To demonstrate conclusively that storage protein RNA localization was dependent on RNA-based sorting mechanism, we analysed transgenic rice plants expressing a β-glucuronidase (GUS) reporter gene containing prolamine or glutelin RNA sequences located at the 3′ UTR of the gene fusion (Fig. 3). GUS-specific primers were used to detect the hybrid RNA by *in situ* RT–PCR. No significant fluorescence signals were observed in control plants (Fig. 3a). While GUS transcripts are localized to the PB-ER in *GUS::prolamine* plants (Fig. 3b), such a distribution pattern was not evident in *GUS::glutelin* plants (Fig. 3c). These results confirm the RNA signal dependence of prolamine RNA localization to the PB-ER.

The exact signal domain responsible for localization of prolamine RNAs to the PB-ER has not been identified, but at least part of the sorting determinant resides in the 3′ UTR. Although prolamine peptide sequences are not required, an AUG initiation codon is essential for RNA localization. This latter observation suggests that prolamine RNA moves as a ribonucleoprotein complex containing many components of the protein synthesis machinery especially factors required for translation initiation, that is, ribosome scanning of the initiation codon. Failure to form the translation initiation complex results in RNA mistargeting. As prolamine protein bodies are closely associated with the cortical cytoskeleton[9], movement of the RNA-translation initiation complex is likely to be mediated by one or more cytoskeletal elements. The transport of ready-to-translate complexes would facilitate the efficient synthesis of large amounts of storage protein on the very restricted PB-ER, a process that probably expedites the formation of the prolamine granule in the ER lumen[3]. □

Methods

T-DNA vector construction and rice transformation

Synthetic prolamine genes were joined after PCR amplification of prolamine coding (CDS), 3′ UTR and glutelin 3′ UTR sequences from pProl14, prolamine 4a, and Gt2 genomic sequences respectively[10]. The HSV or His_6 sequence was added at the end of CDS during PCR. The DNA fragments were inserted downstream of the Gt1 promoter, and the promoter–insert fusion was cloned into the T-DNA transformation vector, pCAMBIA1300. Rice (*Oryza sativa* cv. Kitaake) transformation was performed essentially as described[15]. Transgenic plants were grown in a controlled environment with an 11-hour, 26 °C day and a 13-hour, 22 °C night.

RNA and protein gel blot

Three micrograms of poly(A)$^+$ RNA was resolved on a 1% formaldehyde agarose gel, transferred to a nylon membrane, and hybridized with ^{32}P end-labelled antisense HSV and His_6 oligonucleotides. Immunoblot of seed protein extracts were performed with either HSV monoclonal (Novagen) or His_6 (Invitrogen) antibody and enhanced chemiluminescence substrates (Pierce).

In situ RT–PCR and reverse transcription

Cryosections were prepared from 10–14 day old rice seeds, and fixed on glass slides for 30 min in 2.5% paraformaldehyde, 1.5% glutaraldehyde in 50 mM PIPES buffer, pH 7.2. The sections were then washed with phosphate-buffered saline (PBS) for 15 min followed by water rinses. Fixed sections were overlaid with RT–PCR reaction mixture containing 50 mM Tris-HCl, pH 9.0, 20 mM ammonium sulphate, 2.5 mM $MgCl_2$, 0.2 mM dATP, dCTP and dGTP, 10 μM dTTP, 10 μM Oregon Green 488-dUTP or Alexa 594-dUTP (Molecular Probes), 500 U ml^{-1} MuLV reverse transcriptase (Stratagene), 50 U ml^{-1} *Thermus thermophilus* (Tth) DNA polymerase (Epicentre), and 0.5 μM of each primer (5′-CAGCTC GAGCAGCAATGAAG ATCATTTTCGT-3′ and 5′-GTCGTAGCCAAGACACCGCCAAGGGTGGTA-3′ for prolamine; 5′-GACAAGCTTGTCGGCTTGCGGATAAAGAATAAC-3′ and 5′-CTGGAATTCTAAACAAATACTACTTAAAGGGGT-3′ for glutelin; and 5′-CAGCGAAG AGGCAGTCAACGGGGAA-3′ and 5′-CATTGTTTGCCTCCCTGCTGCGGTT-3′ for GUS). The RT–PCR was allowed to proceed at room temperature for 10 min followed by 60 °C for 20 min. The seed section was then subjected to 8–10 PCR cycles of 95 °C for 1 min, 72 °C for 1 min and 60 °C for 1 min. *In situ* reverse transcription was performed for 3 min at 94 °C, 20 min at 60 °C, and 5 min at 72 °C in the reaction solution containing 50 mM Tris-HCl, pH 9.0, 20 mM ammonium sulphate, 1.25 mM $MgCl_2$, 1 mM $MnSO_4$, PCR enhancer (Epicentre), 50 μM each dATP, dGTP and dCTP, 10 μM dTTP, 20 μM Oregon Green 488-dUTP, 5 mM dithiothreitol, 150 U ml^{-1} RNasin (5′–3′, Inc.), 50 U ml^{-1} Tth DNA polymerase and 0.1 μM reverse primer (5′-GTCAAAGCTTAATCCTCGGGGTCTTCCGGGG-3′ for HSV-tagged plants; and 5′-TCAAGCTTAATGGTGATGGTGATGGTGCAAGA-3′ for His_6-tagged plants). Sections were stained with rhodamine B hexyl ester (final 0.1 μM), $DiOC_6$ (0.5 μM) or propidium iodide (0.5 μM), and then washed with 2 × SSC (0.3 M NaCl, 30 mM sodium citrate) for 15 min, 0.2 × SSC for 15 min twice, and then PBS for at least 10 hours at 4 °C.

Received 30 May; accepted 18 July 2000.

1. Krishnan, H. B., Franceschi, V. R. & Okita, T. W. Immunochemical studies on the role of the Golgi complex in protein body formation in rice seeds. *Planta* **169,** 471–480 (1986).
2. Yamagata, H. & Tanaka, K. The site of synthesis and accumulation of rice storage proteins. *Plant Cell Physiol.* **27,** 135–145 (1986).
3. Okita, T. W. & Rogers, J. C. Compartmentation of proteins in the endomembrane system of plant cells. *Annu. Rev. Plant Physiol. & Plant Mol. Biol.* **47,** 327–350 (1996).
4. Yamagata, H., Tamura, K., Tanaka, K. & Kasai, Z. Cell-free synthesis of rice prolamin. *Plant Cell Physiol.* **27,** 1419–1422 (1986).
5. Li, X., Franceschi, V. R. & Okita, T. W. Segregation of storage protein mRNAs on the rough endoplasmic reticulum membranes of rice endosperm cells. *Cell* **72,** 869–879 (1993).
6. Kim, W. T., Li, X. & Okita, T. W. Expression of storage protein multigene families in developing rice endosperm. *Plant Cell Physiol.* **34,** 595–603 (1993).
7. Li, X. *et al.* Rice prolamine protein body biosynthesis: A BiP-mediated process. *Science* **262,** 1054–1056 (1993).
8. Muench, D. G. *et al.* Molecular cloning, expression and subcellular localization of a BiP homolog from rice endosperm tissue. *Plant Cell Physiol.* **38,** 404–412 (1997).
9. Muench, D. G., Chuong, S. D. X., Franceschi, V. R. & Okita, T. W. Developing prolamine protein bodies are associated with the cortical cytoskeleton in rice endosperm cells. *Planta* **211,** 227–238 (2000).
10. Kim, W. T. & Okita, T. W. Structure, expression, and heterogeneity of the rice seed prolamines. *Plant Physiol.* **88,** 649–655 (1988).
11. Mitsukawa, N. & Tanaka, K. in *Rice Genetics II* (ed. Khush, G. S.) 503–512 (International Rice Research Institute, Manila, Philippines, 1991).
12. Bassell, G. J., Oleynikov, Y. & Singer, R. H. The travels of mRNAs through all cells large and small. *FASEB J.* **13,** 447–454 (1999).
13. Jansen, R. P. RNA-cytoskeletal associations. *FASEB J.* **13,** 455–466 (1999).
14. Dalgleish, G. D., Veyrune, J. L., Accornero, N., Blanchard, J. M. & Hesketh, J. E. Localisation of a reporter transcript by the *c-myc* 3′-UTR is linked to translation. *Nucleic Acids Res.* **27,** 4363–4368 (1999).
15. Hiei, Y., Ohta, S., Komari, T. & Kumashiro, T. Efficient transformation of rice (*Oryza sativa* L.) mediated by *Agrobacterium* and sequence analysis of the boundaries of the T-DNA. *Plant J.* **6,** 271–282 (1994).

Acknowledgements

We thank R. S. Boston and F. Takaiwa for providing the maize BiP antibody and prolamine promoter clone. This work was supported in part by United States Department of Agriculture National Research Initiative Competitive Grant Program, by a National Science Foundation Grant, and by Washington State University College of Agriculture and Home Economics Hatch Project.

Correspondence and requests for materials should be addressed to T.W.O. (e-mail: tokita@wsu.edu).

correction

BcL-2 family proteins regulate the release of apoptogenic cytochrome *c* by the mitochondrial channel VDAC

Shigeomi Shimizu, Masashi Narita & Yoshihide Tsujimoto

Nature **399,** 483–487 (1999).

Figure 1c of this paper was incorrect. The correct figure is reproduced below. □

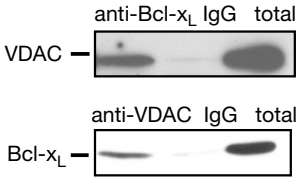

27. Barbet, N., Muriel, W. J. & Carr, A. M. Versatile shuttle vectors and genomic libraries for use with *Schizosaccharomyces pombe*. *Gene* **114,** 59–66 (1992).
28. Moreno, S., Klar, A. & Nurse, P. Molecular genetic analysis of fission yeast *Schizosaccharomyces pombe*. *Methods Enzymol.* **194,** 795–823 (1991).

Acknowledgements. We thank S. O. Sio, Y. Minami and K. Tanaka for comments on the manuscript, M. Yanagida and H. Mukai for helpful suggestions, and Y. Kawabe for technical assistance. This work was supported in part by research grants from the Ministry of Education, Science and Culture of Japan.

Correspondence and requests for materials should be addressed to T.K. (tkuno@kobe-u.ac.jp). The nucleotide sequence of Pek1 has been deposited in DDBJ, EMBL and GenBank under accession number D82023.

Bcl-2 family proteins regulate the release of apoptogenic cytochrome *c* by the mitochondrial channel VDAC

Shigeomi Shimizu*, Masashi Narita & Yoshihide Tsujimoto*

*Osaka University Medical School, Biomedical Research Center, Department of Medical Genetics and *CREST of Japan Science and Technology Corporation (JST), 2-2 Yamadaoka, Suita, Osaka 565-0871, Japan*

During transduction of an apoptotic (death) signal into the cell, there is an alteration in the permeability of the membranes of the cell's mitochondria, which causes the translocation of the apoptogenic protein cytochrome *c* into the cytoplasm, which in turn activates death-driving proteolytic proteins known as caspases[1,2]. The Bcl-2 family of proteins, whose members may be anti-apoptotic or pro-apoptotic, regulates cell death by controlling this mitochondrial membrane permeability during apoptosis[3–5], but how that is achieved is unclear. Here we create liposomes that carry the mitochondrial porin channel (also called the voltage-dependent anion channel, or VDAC) to show that the recombinant pro-apoptotic proteins Bax and Bak accelerate the opening of VDAC, whereas the anti-apoptotic protein Bcl-x_L closes VDAC by binding to it directly. Bax and Bak allow cytochrome *c* to pass through VDAC out of liposomes, but passage is prevented by Bcl-x_L. In agreement with this, VDAC1-deficient mitochondria from a mutant yeast did not exhibit a Bax/Bak-induced loss in membrane potential and cytochrome *c* release, both of which were inhibited by Bcl-x_L. Our results indicate that the Bcl-2 family of proteins bind to the VDAC in order to regulate the mitochondrial membrane potential and the release of cytochrome *c* during apoptosis.

Bax- and Bak-dependent changes in mitochondrial membrane permeability that lead to loss of membrane potential ($\Delta\psi$) and cytochrome *c* release[6–8] are mediated by a polyprotein channel called the permeability transition (PT) pore[6,8,9], which includes VDAC, the adenine nucleotide translocator (ANT) and cyclophilin D (refs 10, 11). VDAC is an abundant protein in the outer mitochondrial membrane which forms a large voltage-gated pore in planar lipid bilayers[12], and acts as the pathway for the movement of substances in and out of the mitochondrion. Bax and Bak interact with the PT pore[8,9]. Bax binds to ANT and can sensitize ANT and PT pores in liposomes to atractyloside, an ANT ligand[9].

During our search for Bcl-x_L-binding proteins in mitochondria using co-immunoprecipitation with an anti-Bcl-x_L antibody, we detected three proteins of relative molecular masses 33K, 18K and 13K (Fig. 1a). Partial amino-acid sequencing of the 33K protein revealed a match with rat VDAC. Co-immunoprecipitation followed by western blot analysis confirmed the interaction between Bcl-x_L and VDAC in isolated mitochondria (Fig. 1b) and also in Bcl-x_L-expressing HepG2 cells (Fig. 1c). No co-immunoprecipitable interaction of Bcl-x_L with Tom 40 (an integral outer-membrane protein) or with F_1-ATPase (an inner-membrane protein) was detected (data not shown), indicating that the interaction between Bcl-x_L and VDAC was specific. As the PT pore is a polyprotein

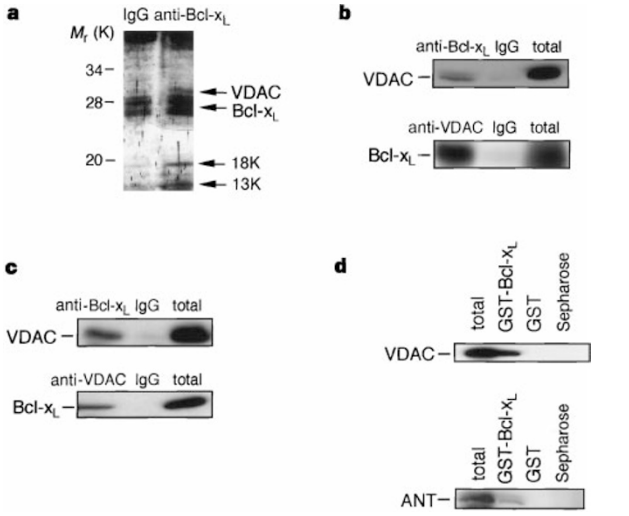

Figure 1 Interaction of Bcl-x_L with VDAC. **a**, Bcl-x_L-binding proteins. Rat liver mitochondria (1 mg ml^{-1}) were incubated with rBcl-x_L (20 mg ml^{-1}) for 5 min and their lysates were immunoprecipitated with anti-Bcl-x_L antibody or rabbit IgG. Immune complexes were analysed by SDS–PAGE and silver staining. **b**, Interaction of rBcl-x_L with VDAC in mitochondria. Mitochondria were incubated with rBcl-x_L, lysed and immunoprecipitated as in **a**, but also with anti-VDAC monoclonal antibody or normal mouse IgG. Anti-VDAC and anti-Bcl-x_L antibodies were used for western blotting. An aliquot of mitochondria (total) was used as the control. **c**, Interaction of rBcl-x_L with VDAC in HepG2 cells. Lysates of human Bcl-x_L-expressing HepG2 cells were immunoprecipitated as for **b**. **d**, Direct interaction between Bcl-x_L and VDAC or ANT. (See Methods for details.) Bound VDAC and ANT were analysed by western blotting; 'total' represents the amount of each protein used.

channel that includes VDAC, co-immunoprecipitation of Bcl-x_L and VDAC from the mitochondria and cells did not necessarily indicate their direct interaction. VDAC purified from rat liver mitochondria efficiently bound to a fusion protein between glutathione-*S*-transferase and Bcl-x_L (GST–Bcl-x_L), however, indicating that Bcl-x_L interacted directly with VDAC; similar results were obtained when recombinant VDAC was used (data not shown). ANT purified from rat heart bound only weakly to GST–Bcl-x_L (Fig. 1d), consistent with earlier observations[9].

As Bcl-x_L binds VDAC, we tested the effect of Bcl-x_L on VDAC activity by using VDAC purified from rat liver mitochondria and reconstituted into liposomes. These VDAC liposomes could take up radiolabelled sucrose, whereas plain or heat-denatured VDAC-containing liposomes could not; uptake was greatly reduced in VDAC liposomes preincubated with a polyanion VDAC inhibitor (Fig. 2a), indicating that this sucrose uptake must be mediated by VDAC. Addition of recombinant (r)Bcl-x_L to VDAC liposomes inhibited VDAC-mediated sucrose uptake in a pH-dependent manner (Fig. 2b): Bcl-x_L functioned at acidic pH, consistent with observations that rBcl-x_L acts as an ion channel in synthetic lipid membranes only under acidic conditions[13–16]. However, when both rBcl-x_L and VDAC were incorporated together into liposomes, Bcl-x_L was able to function at pH 7.3 (Fig. 2c), suggesting that incorporation of Bcl-x_L into the lipid membranes was favoured at lower pH. Although the VDAC has been reported to close below pH 5.0 (ref. 22), our VDAC liposomes showed no difference in behaviour between pH 5.2 and 7.3 (data not shown). VDAC was inhibited by rBcl-x_L in a concentration-dependent manner (Fig. 2d), and two Bcl-x_L mutants (mt-1; F131V, D133A; mt-7; VNW at 135–137 changed to AIL) having partial and no anti-apoptotic activity, respectively[17], gave partial and no inhibition of VDAC-mediated sucrose uptake (Fig. 2d), indicating that those two activities could be linked. As shown in Fig. 2e, mt-1 and mt-7, respectively, bound

VDAC weakly and not at all, indicating that the inhibition of VDAC by Bcl-x_L depends on Bcl-x_L binding to VDAC. VDAC was also inhibited by Bcl-x_L in VDAC liposomes made with recombinant VDAC (Fig. 2f), confirming that VDAC is targeted by Bcl-x_L.

We next tested the effect of Bax on VDAC activity and found that rBax enhanced VDAC-mediated sucrose uptake at pH 5.2 (Fig. 3a), but that uptake of sucrose into plain liposomes incorporating Bax but without VDAC was low (Fig. 3a), indicating that the rBax-enhanced sucrose uptake by VDAC liposomes is mediated not by a putative Bax channel but by the effect of Bax on VDAC. We confirmed this by adding polyanion in the presence of Bax to VDAC liposomes, which significantly inhibited sucrose uptake (Fig. 3a). As the interaction of VDAC and Bax was not inhibited by polyanion (data not shown), and as polyanion inhibited VDAC activity (Fig. 2a) but not Bax channel activity, as assessed by movement of rhodamine 123 (data not shown), we conclude that Bax enhances VDAC activity. Results were similar for VDAC liposomes made with recombinant VDAC, and when pro-apoptotic Bak (lacking the C-terminal 21 amino-acid residues) was used in place of rBax (Fig. 3b). With liposomes containing both rBax and VDAC, Bax could function at pH 7.3 (data not shown). Consistent with the effect of Bax and Bak on VDAC activity, rBax and rBak could bind purified VDAC (Fig. 3c). Binding between endogenous Bax and VDAC occurred in apoptotic but not intact PC12 cells

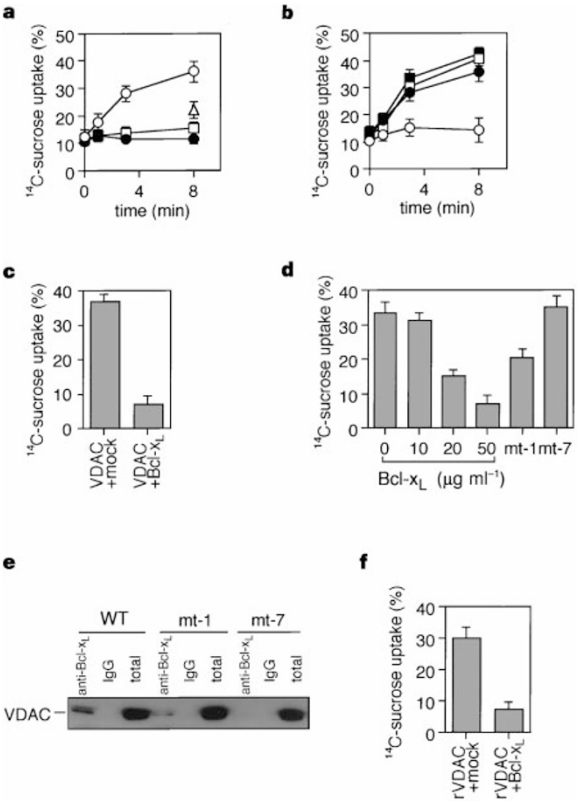

Figure 2 Inhibition of VDAC activity by Bcl-x_L in VDAC liposomes. **a**, Sucrose uptake by VDAC liposomes. Plain liposomes (filled circles), VDAC liposomes (open circles), heat-denaturated VDAC liposomes (open squares), and VDAC liposomes with polyanion (100 μg ml^{-1}) (open triangle) were incubated with ^{14}C-sucrose for the identicated times at pH 5.2 (see Methods). Liposomes were recovered, dissolved in 2% SDS and their ^{14}C-sucrose content counted. **b**, Inhibition of VDAC activity in VDAC liposomes by Bcl-x_L. VDAC liposomes were incubated with ^{14}C-sucrose and either rBcl-x_L (20 μg ml^{-1}) (open symbols) or mock protein (filled symbols) at pH 5.2 (circles) and pH 7.3 (squares), and ^{14}C-sucrose uptake was measured (see Methods). **c**, Inhibition of VDAC activity by Bcl-x_L at neutral pH in liposomes containing VDAC and rBcl-x_L. Purified VDAC and rBcl-x_L were both embedded together into liposomes (see Methods), which were then incubated with ^{14}C-sucrose at pH 7.3 for 3 min and their ^{14}C-sucrose uptake measured. **d**, Inhibition of VDAC activity by Bcl-x_L in a dose-dependent manner and effect of Bcl-x_L mutants. VDAC liposomes were incubated with ^{14}C-sucrose and rBcl-x_L, rBcl-x_L mutant mt-1 or mt-7 protein at 20 μg ml^{-1} at pH 5.2 for 3 min, and ^{14}C-sucrose uptake was measured. **e**, Interaction of Bcl-x_L mutants with VDAC. Experiments as in Fig. 1b were done using rBcl-x_L and rBcl-x_L mutants mt-1 and mt-7. Mitochondrial lysates immunoprecipitated with anti-Bcl-x_L antibody or rabbit IgG were western-blotted with anti-VDAC antibody. WT, wild type. **f**, Inhibition of VDAC activity by Bcl-x_L in liposomes incorporating recombinant VDAC. VDAC liposomes were incubated with ^{14}C-sucrose and rBcl-x_L at pH 5.2 for 3 min and their ^{14}C-sucrose uptake measured.

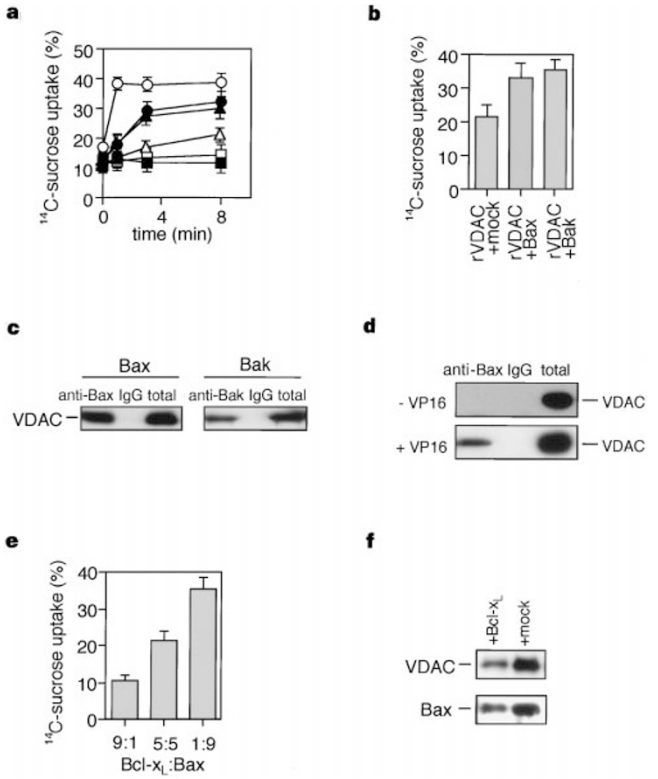

Figure 3 Enhancement of VDAC activity by Bax as well as its inhibition by Bcl-x_L. **a**, ^{14}C-sucrose uptake into VDAC liposomes is enhanced by Bax. Plain liposomes (squares) and VDAC liposomes (circles and triangles) were incubated with ^{14}C-sucrose, rBax (20 μg ml^{-1}) (open circles and open squares), rBax (20 μg ml^{-1}) and polyanion (100 μg ml^{-1}) (open triangles), rBaxΔBH3 (20 μg ml^{-1}) (filled triangles), and mock protein (filled circles and filled squares) at pH 5.2 for the indicated times before measuring ^{14}C-sucrose uptake. **b**, VDAC activity is increased by Bax and Bak in liposomes incorporating recombinant VDAC. VDAC liposomes were incubated with ^{14}C-sucrose and with rBax, rBak or mock protein at pH 5.2 as in **a** and the ^{14}C-sucrose uptake was counted at 3 min. **c**, Direct interaction of Bax and Bak with VDAC. VDAC liposomes preincubated with rBax or rBak were immunoprecipitated with anti-Bax or anti-Bak antibodies or with rabbit IgG and western-blotted with anti-VDAC antibody. An aliquot of the initial mixture (total) was used as control. **d**, Interaction of endogenous Bax with endogenous VDAC in PC12 cells. Lysates from PC12 cells (a rat pheochromocytoma cell line) preincubated with or without 50 μM VP16 for 12 h were immunoprecipitated with either an anti-mouse Bax antibody that crossreacts with rat Bax or rabbit IgG and the immune complexes western-blotted as in **c**. **e**, Antagonism of sucrose import into VDAC liposomes by Bax and Bcl-x_L. VDAC liposomes were incubated with ^{14}C-sucrose and with rBax and rBcl-x_L at the indicated ratios (total 20 μg ml^{-1}) at pH 5.2, and ^{14}C-sucrose uptake measured at 3 min. **f**, Inhibition of interaction with Bax and VDAC by Bcl-x_L. VDAC liposomes incubated with Bcl-x_L or mock protein for 5 min, then with rBax (all at 20 μg ml^{-1}) for 5 min, were immunoprecipitated with anti-Bax (top) or anti-VDAC (bottom) antibodies and western-blotted with anti-Bax or anti-VDAC antibody.

(Fig. 3d). rBax and rBcl-x_L were antagonistic towards VDAC (Fig. 3e). As preincubation of VDAC liposomes with Bcl-x_L significantly inhibited rBax binding to VDAC (Fig. 3f), the effect on VDAC activity of Bax and Bcl-x_L was regulated by their competitive binding to VDAC and their heterodimerization. A recombinant mutant Bax lacking its BH3 region had no effect on VDAC (Fig. 3a), indicating that this region is necessary for enhancing VDAC activity, consistent with our previous observation that the BH3 region is essential for Bak-induced mitochondrial changes[8]. We found that VDAC preparations from rat liver did not contain detectable ANT, as assessed by western blotting, and that sucrose uptake by VDAC liposomes was unaffected by the two ANT ligands atractyloside and bongkrekic acid (data not shown), indicating that we had no contamination by ANT in our VDAC preparations.

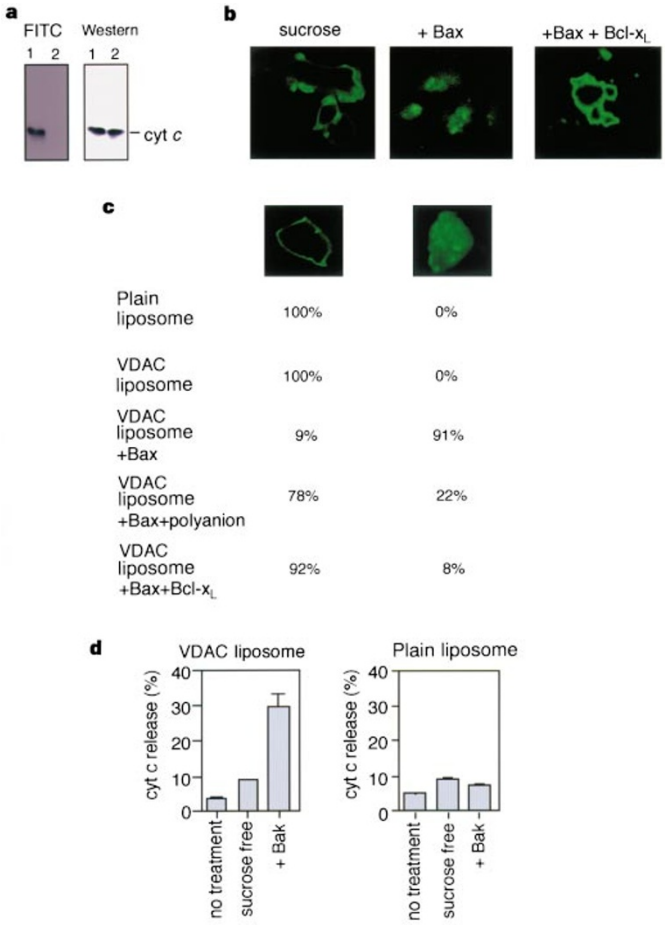

Figure 4 Induction of cytochrome *c* movement through VDAC by Bax and Bak. **a**, FITC labelled cytochrome *c* was run on SDS–PAGE (see Methods) and was detected by fluorescence (left) and western blotting with anti-cytochrome *c* antibody (right): lane 1, FITC–cytochrome *c* (25 pg); lane 2, cytochrome *c* (25 pg). **b**, **c**, Bax-induced import of FITC-cytochrome *c* into VDAC liposomes. VDAC liposomes (**b**, **c**) and plain liposomes (**c**) were incubated with FITC–cytochrome *c* and sucrose (50 mM), plus rBax (52 $\mu g\,ml^{-1}$), rBax (52 $\mu g\,ml^{-1}$) and polyanion (100 $\mu g\,ml^{-1}$), rBax and rBcl-x_L (both at 52 $\mu g\,ml^{-1}$), or without any of these at pH 5.2 for 5 min (see Methods), and were observed under a confocal fluorescence microscope. Representative photographs (original magnification, ×4,800) of VDAC-liposomes are shown in **b**. In **c**, the frequency (given as a percentage) and representative photographs of liposomes with and without influxed cytochrome *c* are shown (original magnification, ×10,000). **d**, Bak-induced cytochrome *c* release form VDAC liposomes. Plain or VDAC liposomes containing 80 mM sucrose and 0.5 mM cytochrome *c* were incubated in sucrose-free buffer with or without rBak for 30 min at pH 5.2 (see Methods). The release of cytochrome *c* was quantified spectrophotometrically (total incorporated cytochrome *c* is 100%).

As Bax and Bak induce cytochrome *c* release through PT pores of isolated mitochondria[6–8] and as they enhance VDAC activity, we investigated whether cytochrome *c* could pass through VDAC in the presence of Bax and Bak. To monitor the movement of cytochrome *c* microscopically, we incubated fluorescein isothiocyanate (FITC)-labelled cytochrome *c* (Fig. 4a) with VDAC liposomes. In the absence of rBax, cytochrome *c* accumulated on the surfaces of plain and VDAC liposomes (Fig. 4b, c), but in the presence of rBax (Fig. 4b, c) or rBak (data not shown), cytochrome *c* accumulated inside VDAC liposomes (Fig. 4b, c). Also, polyanion significantly inhibited Bax-induced cytochrome *c* movement (Fig. 4c), indicating that Bax and Bak allowed cytochrome *c* to pass through VDAC. Bax-induced movement of cytochrome *c* was inhibited in the presence of rBcl-x_L (Fig. 4b, c). When cytochrome *c* and sucrose were initially incorporated inside VDAC liposomes, and the liposomes were then incubated with buffer, a significant amount of cytochrome *c* was released only in the presence of rBak (Fig. 4d) and rBax (data not shown); cytochrome *c* was not released by plain liposomes in the presence of rBak (Fig. 4d). Bax/Bak-dependent passage of cytochrome *c* through VDAC occurred also in the absence of sucrose (data not shown). During these experiments, the number of liposomes did not change, as assessed by flow cytometry (data not shown), and a GST–GFP (green fluorescence protein) fusion protein (M_r = 50K) was not released when rBax was added to VDAC liposomes containing GST–GFP (data not shown), indicating that the liposomes did not rupture and that Bax and Bak enable cytochrome *c* to pass through VDAC.

Our results indicate that Bcl-2 family proteins may target VDAC directly in order to modulate channel activity. We therefore investigated whether VDAC could be a target for Bcl-2 family proteins that are involved in regulating the apoptosis-associated loss of mitochondrial membrane potential ($\Delta\psi$) and the release of cytochrome *c*. As no mammalian cells lacking VDAC were available and because Bcl-2 family proteins can function in yeast cells[18,19], we used a yeast mutant deficient in VDAC1 (ΔVDAC)[20] and found that mitochondria isolated from the wild-type yeast lost $\Delta\psi$ and released cytochrome *c* after addition of rBax in a dose-dependent manner (Fig. 5a, d) like mammalian mitochondria, whereas rBax did not cause a loss of $\Delta\psi$ and cytochrome *c* release in mitochondria isolated from ΔVDAC yeast cells (Fig. 5b, d). However, rBax did induce both effects in mitochondria from ΔVDAC yeast transfected with the human (h) *vdac1* gene (Fig. 5c, d), indicating that the failure of ΔVDAC yeast mitochondria to respond to rBax was due to the absence of functional VDAC. Bax-mediated $\Delta\psi$ loss and cytochrome *c* release in yeast mitochondria were inhibited by rBcl-x_L (Fig. 5a, c, d). Results were similar when rBak was used (Fig. 5a–c, and data not shown). These results indicate that Bcl-2 family proteins target VDAC to regulate apoptosis-associated mitochondrial loss of $\Delta\psi$ and release of cytochrome *c*.

The fact that Bax and Bak enable cytochrome *c* to pass through VDAC, whereas Bcl-x_L does not, may explain how cytochrome *c* is released during apoptosis. We used the VDAC1-deficient yeast mutant[20] to show that VDAC is essential for Bax/Bak-induced mitochondrial $\Delta\psi$ loss and cytochrome *c* release. Although yeast cells carry VDAC1 and VDAC2, VDAC2 makes only a small contribution to the membrane permeability to metabolites.[21] Extrapolation of these observations suggests that VDAC is essential for cytochrome *c* release during apoptosis of mammalian cells. The estimated size of the VDAC pore is ~2.6 nm, which is not large enough for folded cytochrome *c* with a similar diameter to pass through VDAC[22]; indeed, VDAC liposomes did not allow the passage of cytochrome *c* (Fig. 4). Therefore Bax/Bak probably induces a conformational change in VDAC so that cytochrome *c* can pass through the channel, although it is possible that Bax/Bak and VDAC could together form a larger channel, and other unknown mechanisms may contribute to apoptotic cytochrome *c* release *in vivo*.

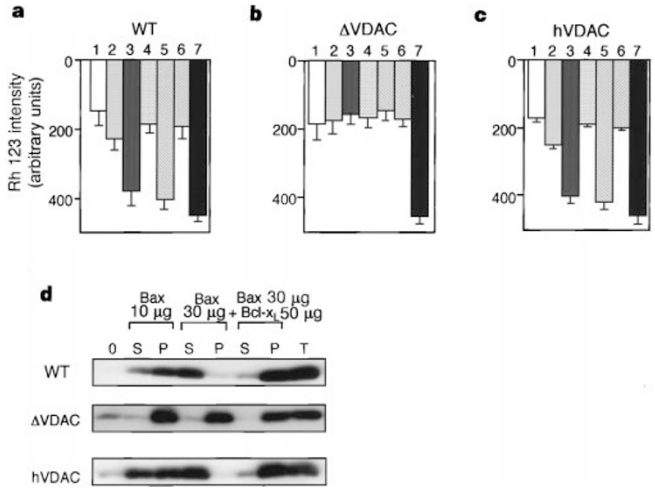

Figure 5 Requirement of VDAC for Bax/Bak-induced loss of membrane potential and cytochrome *c* release in yeast mitochondria. **a**–**c**, Inability of VDAC-deficient mitochondria to show rBax/rBak-induced loss of membrane potential. Mitochondria (1.0 mg ml^{-1}) isolated from wild-type (WT) yeast (**a**), VDAC1-deficient yeast (ΔVDAC) (**b**), or human VDAC1-expressing ΔVDAC (hVDAC) (**c**) yeast were incubated with: lane 2, 10 μg ml^{-1}, and lanes 3, 4, 30 μg ml^{-1} rBax; lanes 5, 6, 30 μg ml^{-1} rBak; lane 1, mock, in the presence (lanes 4, 6) or absence (lanes 3, 5) of 50 μg ml^{-1} of Bcl-x$_L$ for 10 min, and Δψ was measured by rhodamine (Rh) 123 intensity; lane 7, complete loss of Δψ was demonstrated by incubation of mitochondria with 1 mM CCCP for 10 min. **d**, Failure of VDAC1-deficient mitochondria to show Bax-induced cytochrome *c* release. Mitochondria (1 mg ml^{-1}) isolated from wild-type, ΔVDAC or hVDAC1-expressing ΔVDAC yeasts (hVDAC) were incubated with rBax (10 and 30 μg ml^{-1}) either with or without rBcl-x$_L$ (50 μg ml^{-1}) for 10 min, then centrifuged: supernatants (S) and pellets (P) were western-blotted with anti-yeast cytochrome *c* antibody. '0', Supernatant of mitochondria before treatment; 'T', unspun mitochondria . Data are representative of three independent experiments.

Bax and Bcl-2 have been shown to interact with ANT and Bax to sensitize ANT to its atractyloside ligand in ANT liposomes and in partially purified PT-pore liposomes[9]. However, Bax did not affect mitochondrial ADP uptake, which is mediated by ANT (our unpublished observations). Therefore Bax might modulate ANT activity after binding under certain circumstances, but our results strongly indicate that VDAC is a functional target for Bcl-2 family proteins. As Bax/Bak induces loss of Δψ across the inner membrane in mitochondria and as the PT pore is a polyprotein channel, the Bax/Bak-mediated conformational change of VDAC probably affects other channels in the PT pore that control inner-membrane permeability. Alternatively, interaction of Bax/Bak with ANT or ANT-related channels in the inner membrane might be directly involved in Δψ collapse. As PT inhibitors such as cyclosporin A and bongkrekic acid can inhibit Bax/Bak-induced cytochrome *c* release in isolated mitochondria[6,8], VDAC-mediated cytochrome *c* release could be controlled not only by Bcl-2 family proteins but also by other components of the PT pore such as ANT (a target of bongkrekic acid) and cyclophilin D (a target of cyclosporin A). Thus, various components of the PT pore seem to interact with each other. The interaction of Bcl-x$_L$ and Bax with ANT may direct these molecules to bind antagonistically with VDAC inside the PT pore rather than with VDAC in isolation.

Taken together, our results indicate that the Bcl-2 family of proteins target VDAC to regulate apoptosis-associated mitochondrial changes that are central to determining the survival or death of cells. □

Methods

Antibodies. Anti-pigeon cytochrome *c* monoclonal antibody (7H8.2C12), anti-yeast cytochrome *c* polyclonal antibody and anti-rat ANT polyclonal antibody were kindly provided by E. Margoliash, G. Shatz and H. H. Schmid, respectively. Anti-human VDAC monoclonal antibody (31HL), which cross-reacts with rat VDAC, was from Calbiochem. Anti-human Bcl-x$_L$ (L19), anti-human Bak (G23) and anti-human Bax (N20) polyclonal antibodies were from Santa Cruz Biotechnology.

Immunoprecipitation and western blot analysis. Rat liver mitochondria were isolated as described[23]. Immunoprecipitation was done as described[8] using cells, mitochondria and liposomes lysed and sonicated in lysis buffer (10 mM HEPES, pH 7.4, 142.5 mM KCl, 5 mM $MgCl_2$, 1 mM EGTA, 0.5% N-P40) containing proteinase inhibitors. To detect binding between purified proteins, VDAC (0.2 μg) and ANT (0.2 μg) were incubated for 3 h either with GST-Bcl-x$_L$ (0.2 μg) or GST (0.2 μg) in 100 μl of the lysis buffer. Then, these proteins were incubated with glutathione (GSH)–Sepharose or Sepharose for 3 h. After brief centrifugation, beads were washed and resuspended in sample buffer for SDS–PAGE.

Protein purification. Human Bcl-x$_L$, two Bcl-x$_L$ mutants, human Bak (lacking the C-terminal 21 amino-acid residues), human Bax, Bax lacking the BH3 region (BaxΔBH3), and mock proteins were produced and purified as described[8]. Haemagglutinin (HA)-tagged human VDAC1 was expressed in *Escherichia coli* strain DE3 using the Xpress System (Invitrogen) and purified on an HA column. All proteins except for VDAC were dissolved in 10 mM HEPES-K$^+$ (pH 7.4) with 1 mM DTT, and VDAC was in VDAC buffer (10 mM Tris-Cl, pH 7.0, 1 mM EDTA, and 3% Triton-X100).

Rat liver VDAC was purified as described[24]. Rat heart ANT was purified as described[25]. The purity of VDAC and ANT was shown to be >95%.

Reconstitution of VDAC in liposomes. Purified and recombinant VDAC were reconstituted in small unilamelar vesicles by a modification of the sonic freeze–thaw procedure[26]. Briefly, 100 mg phospholipid (soybean, type II-S) was dissolved into 1 ml liposome medium containing 30 mM sodium sulphonate and 20 mM Tricine-NaOH (pH 7.3 or pH 5.2) with or without 80 mM sucrose. After sonication, purified or recombinant VDAC protein (200 μg) was added with or without rBcl-x$_L$ (200 μg) and rBax (200 μg), and this suspension was subjected to two freeze–thaw cycles. Heat-denatured VDAC protein was obtained by heating at 95 °C for 10 min. Then unilamelar VDAC liposomes were produced by mild sonication and fractionated on Sephadex G-50 columns. Light scattering from each fraction was measured spectrophotometrically at 520 nm, and the fraction containing 700–900 arbitrary units per μl was used.

A sucrose-import experiment was performed by measuring ^{14}C-sucrose uptake. Liposomes (10 μl) were incubated with 5 μl ^{14}C-sucrose (97%; 200 μCi ml^{-1}) at 25 °C and filtered by centrifugation using a 30K limiting filter (Millipore) to remove free ^{14}C-sucrose; incorporated ^{14}C-sucrose was measured in a gamma-scintillation counter (Wallac 1414).

Cytochrome *c* translocation experiment. FITC-labelled cytochrome *c* was produced as described[27]: the FITC/cytochrome *c* molar ratio was 0.47. FITC-labelled cytochrome *c* was detected with a lumino-image analyser (LAS-1000, Fujifilm). Liposomes (2 μl) were incubated with both sucrose (50 mM) and

FITC-labelled cytochrome *c* (50 μM) and various proteins in a total volume of 29 μl at pH 5.2; labelled cytochrome *c* was visualized using confocal microphotography (LSM-745, Olympus).

For cytochrome *c* export, liposomes (1 ml) in sucrose (80 mM)-containing buffer were mixed with cytochrome *c* (100 μM) and freeze-thawed for two cycles. After unilamerization, 20 μl liposomes were incubated with 1 ml sucrose-free buffer with or without 20 μg ml^{-1} rBak for 10 min at 25 °C, then filtered by centrifugation through a 30K filter to separate liposomes from free cytochrome *c*. Free cytochrome *c* was determined from the absorbance at 408 nm.

Yeast mitochondria. A VDAC1-deficient yeast strain (ΔVDAC; M22-2) and its parent strain (M3) were used. A human VDAC1-expressing ΔVDAC yeast strain was produced by transfecting human *vdac1* cDNA using lithium acetate. Mitochondria were isolated essentially as described[28], using zymolyase 20T to form spheroplasts which were then homogenized. Isolated mitochondria were suspended in 0.3 M mannitol, 10 mM Tris–maleiate (pH 7.4), 0.2 mM EDTA, 0.05% BSA (yMt buffer). Mitochondria (0.5 mg ml^{-1}) were incubate at 25 °C in yMT buffer plus 4.2 mM succinate. $\Delta\psi$ was measured by following the uptake of rhodamine 123 (Rh123) as described[23]. For detecting the release of cytochrome *c*, mitochondria were spun, and the supernatants and pellets were western-blotted with anti-yeast cytochrome *c* antibodies.

Received 15 January; accepted 1 April 1999.

1. Thornberry, N. A. & Lazebnik, Y. Caspases: Enemies within. *Science* **281,** 1312–1316 (1998).
2. Green, D. R. & Reed, J. C. Mitochondria and apoptosis. *Science* **281,** 1309–1312 (1998).
3. Merry, D. E. & Korsmeyer, S. J. Bcl-2 gene family in the nervous system. *Annu. Rev. Neurosci.* **20,** 245–267 (1997).
4. Adams, J. M. & Cory, S. The Bcl-2 protein family: arbiters of cell survival. *Science* **281,** 1322–1326 (1998).
5. Tsujimoto, Y. Role of Bcl-2 family proteins in apoptosis: apoptosomes or mitochondria? *Genes to Cells* **3,** 697–707 (1998).
6. Jürgensmeier, J. M. *et al.* Bax directly induces release of cytochrome c from isolated mitochondria. *Proc. Natl Acad. Sci. USA* **95,** 4997–5002 (1998).
7. Eskes, R. *et al.* Bax-induced cytochrome *c* release from mitochondria is independent of the permeability transition pore but highly dependent on Mg^{2+} ions. *J. Cell Biol.* **143,** 217–224 (1998).
8. Narita, M. *et al.* Bax interacts with the permeability transition pore to induce permeability transition and cytochrome *c* release in isolated mitochondria. *Proc. Natl Acad. Sci. USA* **95,** 14681–14686 (1998).
9. Marzo, I. *et al.* Bax and adenine nucleotide translocator cooperate in the mitochondrial control of apoptosis. *Science* **281,** 2027–2031 (1998).
10. Bernardi, P., Broekemeier, K. M. & Pfeiffer, D. R. Recent progress on regulation of the mitochondrial permeability transition pore; a cyclosporin-sensitive pore in the inner mitochondrial membrane. *J. Bioenerg. Biomembr.* **26,** 509–517 (1994).
11. Zoratti, M. & Szabó, I. The mitochondrial permeability transition. *Biochim. Biophys. Acta* **1241,** 139–176 (1995).
12. Colombini, M. Voltage gating in the mitochondrial channel, VDAC. *J. Membr. Biol.* **111,** 103–111 (1989).
13. Antonsson, B. *et al.* Inhibition of Bax channel-forming activity by Bcl-2. *Science* **277,** 370–372 (1997).
14. Minn, A. J. *et al.* Bcl-x_L forms an ion channel in synthetic lipid membranes. *Nature* **385,** 353–357 (1997).
15. Schendel, S. L. *et al.* Channel formation by antiapoptotic protein Bcl-2. *Proc. Natl Acad. Sci. USA* **94,** 5113–5118 (1997).
16. Schlesinger, P. H. *et al.* Comparison of the ion channel characteristics of proapoptotic Bax and antiapoptotic Bcl-2. *Proc. Natl Acad. Sci. USA* **94,** 11357–11362 (1997).
17. Cheng, E. H., Levine, B., Boise, L. H., Thompson, C. B. & Hardwick, J. M. Bax-independent inhibition of apoptosis by Bcl-x_L. *Nature* **379,** 554–556 (1996).
18. Greenhalf, W., Stephan, C. & Chaudhuri, B. Role of mitochondria and C-terminal membrane anchor of Bcl-2 in Bax induced growth arrest and mortality in *Saccharomyces cerevisiae*. *FEBS Lett.* **380,** 169–175 (1996).
19. Matsuyama, S., Xu, Q., Velours, J. & Reed, J. C. The mitochondrial F_OF_1-ATPase proton pump is required for function of the proapoptotic protein Bax in yeast and mammalian cells. *Mol. Cell* **1,** 327–336 (1998).
20. Blachly-Dyson, E., Peng, S., Colombini, M. & Forte, M. Selectivity changes in site-directed mutants of the VDAC ion channel: structural implications. *Science* **247,** 1233–1236 (1990).
21. Lee, A. C., Xu, X., Blachly-Dyson, E., Forte, M. & Colombini, M. The role of yeast VDAC genes on the permeability of the mitochondrial outer membrane. *J. Membr. Biol.* **161,** 173–181 (1998).
22. Mannella, C. A. Conformational changes in the mitochondrial channel protein, VDAC, and their functional implications. *J. Struct. Biol.* **121,** 207–218 (1998).
23. Shimizu, S. *et al.* Bcl-2 prevents apoptotic mitochondrial dysfunction by regulating proton flux. *Proc. Natl Acad. Sci. USA* **95,** 1455–1459 (1998).
24. DePinto, V., Prezioso, G. & Palmieri, F. A simple and rapid method for the purification of the mitochondrial porin from mammalian tissues. *Biochem. Biophys. Acta* **905,** 499–502 (1987).
25. Rück, A., Dolder, M., Wallimann, T. & Brdiczka, D. Reconstituted adenine nucleotide translocase forms a channel for small molecules comparable to the mitochondrial permeability transition pore. *FEBS Lett.* **426,** 97–101 (1998).
26. Báthori, G., Sahin-Tóth, M., Fonyó, A. & Ligeti, E. Transport properties and inhibitor sensitivity of isolated and reconstituted porin differ from those of intact mitochondria. *Biochem. Biophys. Acta* **1145,** 168–176 (1993).
27. Kelvin, H. & Fowlkes, B. J. in *Current Protocols in Immunology* 5.3.1–5.3.11 (Wiley Interscience, New York, 1990).
28. Daum, G., Bohni, P. C. & Schatz, G. Import of proteins into mitochondria. Cytochrome b2 and cytochrome c peroxidase are located in the intermembrane space of yeast mitochondria. *J. Biol. Chem.* **257,** 13028–13033 (1982).

Acknowledgements. We thank E. Margoliash, G. Schatz and H. H. Schmid for antibodies against pigeon cytochrome *c*, yeast cytochrome *c*, and rat ANT, respectively; M. Forte for VDAC1-deficient yeast (M22-2), its wild type (M3), and human *vdac1* cDNA; J. M. Hardwick for Bcl-x_L mutant cDNAs; M. Colombini for the polyanion; T. Chittenden for the expression plasmid for the GST–Bak fusion protein; and N. Tsujimoto for editorial assistance. This study was supported by grants for Scientific Research on Priority Areas, for Center of Excellence Research and for Scientific Research, from the Ministry of Education, Science, Sports and Culture of Japan.

Correspondence and requests for materials should be addressed to Y.T. (e-mail: tsujimot@gene.med.osaka-u.ac.jp).

Interaction of E1 and hSNF5 proteins stimulates replication of human papillomavirus DNA

Daeyoup Lee*, Hekwang Sohn*, Ganjam V. Kalpana† & Joonho Choe*

** Department of Biological Sciences, Korea Advanced Institute of Science and Technology, Taejon 305-701, Korea*

† Department of Molecular Genetics, Albert Einstein College of Medicine, Bronx, New York 10461, USA

Mammalian viruses often use components of the host's cellular DNA replication machinery to carry out replication of their genomes, which enables these viruses to be used as tools for characterizing factors that are involved in cellular DNA replication. The human papillomavirus (HPV) E1 protein is essential for replication of the virus DNA[1–3]. Here we identify the cellular factor that participates in viral DNA replication by using a two-hybrid assay[4] in the yeast *Saccharomyces cerevisiae* and E1 protein as bait. Using this assay, we isolated Ini1/hSNF5 (ref. 5), a component of the SWI/SNF complex which facilitates transcription by altering the structure of chromatin[6]. *In vitro* binding and immunoprecipitation confirmed that E1 interacts directly with

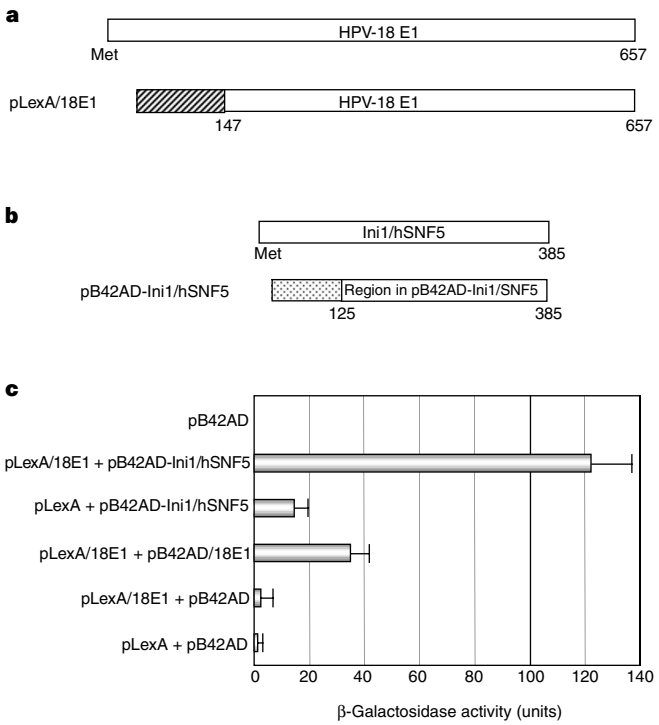

Figure 1 Interaction between HPV-18 E1 and Ini1/hSNF5 proteins. **a**, Structure of the pLexA/18E1 plasmid. Bar represents the LexA DNA binding domain for the LexA operator. **b**, Structure of pB42AD-Ini1/hSNF5. The dotted region represents an activation domain for a yeast promoter. **c**, Quantification of yeast two-hybrid interactions. Values represent the average for five different EGY48 colonies co-expressing the specified fusion proteins. Error bars indicate the standard deviation for each sample.